

# ZnO nanowires with high aspect ratios grown by metalorganic chemical vapor deposition using gold nanoparticles

Sang-Woo Kim<sup>a)</sup> and Shizuo Fujita<sup>b)</sup>

*International Innovation Center, Kyoto University, Kyodai-Katsura, Nishikyo-ku, Kyoto 615-8510, Japan*

Shigeo Fujita

*Department of Electronic Science and Engineering, Kyoto University, Kyodai-Katsura, Nishikyo-ku, Kyoto 615-8510, Japan*

(Received 19 April 2004; accepted 24 January 2005; published online 7 April 2005)

ZnO nanowires with diameters ranging from 20 to 60 nm and lengths in the range 5–15  $\mu\text{m}$  were synthesized by metalorganic chemical vapor deposition, assisted by colloidal gold nanoparticles with a diameter of 20 nm dispersed on  $\text{SiO}_2/\text{Si}$  substrates. The ZnO nanowires were found to have a high-internal quantum efficiency and negligibly weak deep-level emission, as evidenced by photoluminescence measurements. The clear observation of free-exciton and biexciton emission indicates that the ZnO nanowires prepared by this method are of high quality. © 2005 American Institute of Physics. [DOI: 10.1063/1.1883320]

ZnO nanostructures have been studied extensively.<sup>1–3</sup> In particular, quasi-one-dimensional ZnO nanostructures such as nanowires,<sup>2</sup> nanobelts,<sup>4</sup> and nanorods<sup>5</sup> have been a subject of considerable interest for potential applications in multifunctional nanodevices such as ultraviolet nanolasers and nanosensors. A number of groups have reported on the fabrication of ZnO nanowires with high aspect ratios using vapor-liquid-solid (VLS) processes<sup>2,6,7</sup> and thermal evaporation techniques.<sup>4,8,9</sup> However, in such methods, high temperature processes of over 900 °C are typically required for their successful formation. This seriously limits the applicable substrate materials and enhances thermal strain and damage in the structures. Moreover, a deep-level emission band is usually observed in ZnO nanowires grown by the abovementioned methods,<sup>6–9</sup> indicating that they contain a number of point defects.

ZnO nanorods with very weak deep-level emission, grown by metalorganic chemical vapor deposition (MOCVD), have been reported without the aid of a catalyst at low growth temperatures (e.g., 300–500 °C).<sup>5,10,11</sup> However, the realization of ZnO nanowires with the high aspect ratios of narrow diameters (several tens of nm) and large lengths (a few  $\mu\text{m}$  ~ a few tens of  $\mu\text{m}$ ) by MOCVD using self-assembly is not facilitated because the height and the width of a nanorod structure in the initial stage simultaneously increases with growth time even though ZnO has a preferred *c*-axis growth property.

Jo *et al.* recently reported on the formation of ZnO nanowires having an average diameter of 60 nm and a length of 5–20  $\mu\text{m}$  on gold (Au) nanoparticles, which act as a catalyst, using the thermal evaporation/condensation method.<sup>12</sup> This method is very promising because it permits the density of ZnO nanowires to be effectively controlled. However, a high temperature (e.g., 950–1000 °C) process is also required in this method. In this work, ZnO nanowires with high aspect ratios were synthesized by MOCVD by means of assistance by Au nanoparticles at a MOCVD-growth temperature of 550 °C. The resulting ZnO nanowires showed a high-internal

quantum efficiency and negligibly weak deep-level emission in photoluminescence (PL) measurements. In addition, free-exciton and biexciton emissions were clearly observed from the ZnO nanowires.

A commercially available colloidal solution of Au nanoparticles with an average diameter of 20 nm was spin-coated onto  $\text{SiO}_2/\text{Si}$  substrates. The substrates for the growth of the ZnO nanowires were prepared by three iterations of a “spin-coating and air-drying” onto the  $\text{SiO}_2/\text{Si}$  substrates. The MOCVD growth of ZnO was carried out on the substrates at a pressure of 200 Torr for 30 min. Typical flow rates of source materials, diethylzinc (DEZn), and  $\text{N}_2\text{O}$ , were 2 and 1250  $\mu\text{mol}/\text{min}$ , respectively. MOCVD-growth temperatures of 400, 550, and 900 °C were employed.

Figures 1(a) and 1(b) show field-emission scanning electron microscope (FE-SEM) images of Au nanoparticles with a density of about  $4.1 \times 10^9 \text{ cm}^{-2}$  dispersed on the  $\text{SiO}_2/\text{Si}$  substrate and ZnO nanowires grown at 550 °C on the substrate shown in Fig. 1(a), respectively. Although a number of Au nanoparticles are lumped together, the dispersion of the Au nanoparticles on the  $\text{SiO}_2/\text{Si}$  substrate is fairly good, as shown in Fig. 1(a). Figure 1(b) shows uniform ZnO nanowires entangled on the substrate. The diameters of the nanowires were in the range from 20 to 60 nm and their lengths were 5–15  $\mu\text{m}$ , showing their high aspect ratios. The density of the MOCVD-grown ZnO nanowires shown in Fig. 1(b) is somewhat comparable to that of Au nanoparticles dispersed on the  $\text{SiO}_2/\text{Si}$  substrate.<sup>13</sup>

As shown in Fig. 2(a), the nanowires grown at 550 °C are basically comprised of hexagonal facets and ball-shaped Zn–Au alloys on the top faces of the nanowires are barely observed unlike other reported metal-catalyst-driven VLS-growth methods. In addition, no characteristic peaks corresponding to Au from the top face of the nanowires marked by a circle in Fig. 2(a) are evident in the energy-dispersive x-ray (EDX) spectrum shown in Fig. 2(b).

At a growth temperature of 400 °C, vertically well-aligned ZnO nanorods were formed on the Au nanoparticle-dispersed substrate [Fig. 2(c)]. The heights and the widths of the nanorods are in the range of 540–600 nm and 80–180 nm, respectively. However, no significant differences between the ZnO nanorods on the Au nanoparticle-dispersed

<sup>a)</sup>Present address: Nanoscience Centre, University of Cambridge, 11 J. J. Thomson Ave., Cambridge CB3 0FF, UK.

<sup>b)</sup>Electronic mail: fujita@iic.kyoto-u.ac.jp

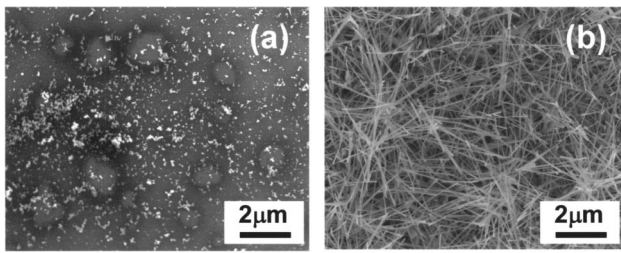


FIG. 1. (a) Plan-view FE-SEM images of Au nanoparticles on a SiO<sub>2</sub>/Si substrate. (b) ZnO nanowires grown on (a) at 550 °C.

substrate and those on a bare SiO<sub>2</sub>/Si substrate were observed, indicating that the nucleation of ZnO for the rod structure on the SiO<sub>2</sub> surface<sup>11</sup> governs the entire growth of ZnO rather than nucleation of ZnO, assisted by Au nanoparticles at the growth temperature 400 °C. On the other hand, flower-like ZnO structures were densely grown at 550 °C on a bare SiO<sub>2</sub>/Si substrate without Au nanoparticles. This strongly suggests that Au nanoparticles play an important role in the formation of ZnO nanowires at this growth temperature of 550 °C. As shown in Fig. 2(d), ZnO nanowires with Au-alloyed tips were fabricated on the Au nanoparticle-dispersed substrate at 900 °C, clearly indicating that the formation of ZnO nanowires by MOCVD at the high growth temperature of 900 °C is mainly the result of a VLS process. The specific role of Au nanoparticles in the formation of the ZnO nanowires by MOCVD will be studied in detail in a further study.

The optical properties of the nanowires were characterized by PL measurements. The ZnO-nanowire sample shown in Fig. 1(b) was used for the PL measurements. The temperature dependencies of the spectra and integrated intensity of the PL are shown in Figs. 3(a) and 3(b), respectively. The peak labeled “EX” (3.375 eV) and another peak labeled “D<sup>0</sup>X” (3.362 eV) can be attributed to free exciton and neutral donor-bound exciton emission, respectively. The emission bands labeled “EX-1LO and EX-2LO” originate from the radiative recombination of the first and second longitudinal optical (LO) phonon replicas of free excitons, respectively, considering an energy separation for each emission band of about 64 meV.<sup>14</sup> This ZnO-nanowire sample exhibited a negligible deep-level emission band in all temperature ranges examined (not shown).

As mentioned in the first paragraph of this letter, a number of groups have reported the deep-level emission associated with point defects in their ZnO nanostructures.<sup>6–9</sup> Very recently, Shalish *et al.* showed that the size reduction of ZnO nanowires on Si using a mixture of ZnO and graphite powders as the growth source causes more atoms to be closer to the surface, resulting in a surface-luminescence (deep-level emission) increase at the expense of band-edge emission.<sup>15</sup> It is noteworthy that most reports on the optical properties of MOCVD-grown ZnO nanorods<sup>5,10,11</sup> and nanowires (this work) point out that the deep-level emission band is very weak, almost negligible, compared with the band-edge emission even at RT. From this comparison, it would appear that MOCVD-growth is an efficient method for producing high-quality ZnO nanostructures with less-sensitive surface states.

As the temperature is increased, the EX band becomes dominant compared to the D<sup>0</sup>X band due to the thermal dissociation of donor-bound-excitons. In typical ZnO films or bulk crystals, the EX band is not clearly observed at low

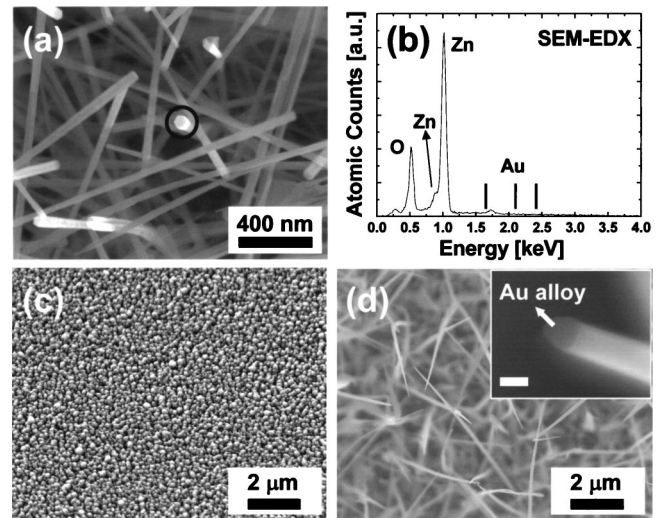


FIG. 2. (a) High-resolution plan-view FE-SEM image of ZnO nanowires grown at 550 °C; (b) SEM-EDX spectrum recorded from the top surface [the point marked by a circle in (a)] of a single nanowire; (c) and (d) show ZnO nanorods (FE-SEM image taken at a tilt angle of 45°) and nanowires (plan-view FE-SEM image) grown on the substrate represented at Fig. 1(a) at 400 and 900 °C, respectively; (d) is a FE-SEM image of a tip area in one of the nanowires grown at 900 °C. Scale bar in the inset indicates 50 nm.

temperatures due to the localization of excitons by impurities (especially donors). At higher temperatures, usually over 70 K, the EX band is predominant because of the ionization of impurities that are used to bind excitons at low temperatures.<sup>14</sup> The clear observation of the dominant EX band in the emission spectrum, even at a temperature as low as 50 K, as well as the fact that the EX peak remains as a shoulder of the D<sup>0</sup>X peak at 10 K, suggests that low levels of impurities were incorporated in the sample. The intensity ratio ( $I_{10\text{ K}}/I_{300\text{ K}}$ ) of the integrated luminescence intensity between 10 and 300 K was 7.6, which is much lower than the case of ZnO thin films on either Si or Al<sub>2</sub>O<sub>3</sub> substrates (in our samples,<sup>14</sup>  $I_{10\text{ K}}/I_{300\text{ K}} > 100$ ). It should be noted that the integrated luminescence intensity is largely unchanged (10–30 K) and the near-band edge emission as a main emission band (negligibly weak deep-level emission as already mentioned) is very strong in all temperature ranges examined in the PL measurements. In the above characteristics, similarly to the previous publications,<sup>16,17</sup> one may assume that all of the carriers radiatively recombine at 10 K and the internal quantum efficiency at 300 K is derived by the integral intensity ratio as  $I_{300\text{ K}}/I_{10\text{ K}} \times 100(\%)$ . Thus, the internal quantum efficiency of the ZnO-nanowire sample is estimated to be about 13% at 300 K, which is comparable to that of ZnO nanoparticles.<sup>18</sup> The clear observation of the EX band even at low temperatures and the high-internal quantum efficiency could be due to enlarged surface areas emitting photons by nanostructuring and the formation of an individual ZnO nanowire with a lower density of defects, such as a dislocation, compared with that of a ZnO thin film.

Figure 4 shows PL spectra obtained for ZnO nanowires under various excitation densities at 77 K. The PL spectra under high excitation were obtained using a mode-locked Ti:Al<sub>2</sub>O<sub>3</sub> laser with a repetition rate of 80 MHz and a 1 kHz regenerative amplifier (REGEN). The output pulse of the REGEN has a pulse duration of about 150 fs at a wavelength of 796 nm. The pump pulse of 330 nm obtained from an optical parametric amplifier (OPA) was used in this experi-

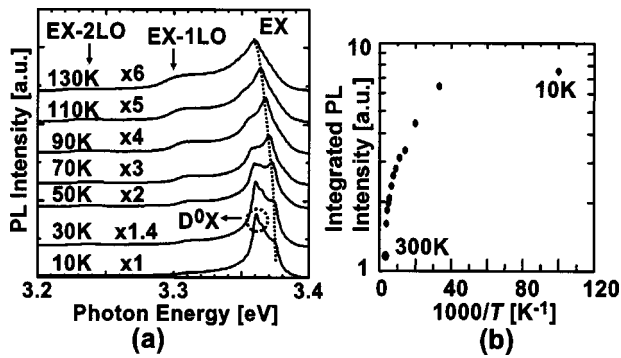


FIG. 3. (a) Band-edge PL spectra of, at various temperatures, for the ZnO-nanowire sample [shown in Fig. 1(b)]. With an increase in temperature, the EX band becomes clear, while the intensity of the  $D^0X$  peak gradually decreases; (b) integrated PL intensity as a function of temperature.

ment. EX and  $D^0X$  bands are clearly observed in the PL spectrum excited by a He–Cd laser at 77 K. As the excitation density increases, a new emission band labeled “BX” appears at 3.35 eV. The PL-integrated intensity of the EX band exhibited a linear dependence on the excitation density ( $I_{EX} \propto I_{EXC}^{1.06}$ ), while that of the emission band BX grew superlinearly with respect to the excitation density ( $I_{BX} \propto I_{EXC}^{1.34}$ ). In addition, the energy separation of the two peaks EX and BX was 20 meV in the PL spectrum, which is in general agreement with the reported value of 12–20 meV for the biexciton binding energy of ZnO.<sup>19–21</sup> From the experimental results, we conclude that the origin of the broad BX band is from the radiative recombination of biexcitons.

The result showing that the luminescence intensity of the BX band with the excitation power density follows  $I_{BX} \propto I_{EXC}^{1.34}$  indicates that the biexciton density does not vary with the square of the exciton density. One of the reasons for the reduction in the exponent from 2 could be explained by considering the short recombination time of excitons and biexcitons in direct-band-gap materials.<sup>22,23</sup> The radiative lifetime of biexcitons is shorter than that of excitons, resulting in the absence of any quadratic dependence of biexciton density as a function of exciton density. For other reasons, the reduction in the exponent might be also due to the  $D^0X$

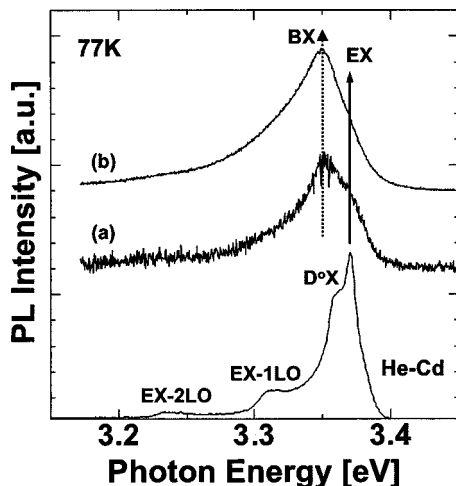


FIG. 4. PL spectra measured at 77 K under various excitation intensities. The bottom most curve shows a PL spectrum obtained using a He–Cd (325 nm) laser. The remaining curves show PL spectra under high excitation obtained by a mode-locked Ti:Al<sub>2</sub>O<sub>3</sub> laser with a repetition rate of 80 MHz and 1 kHz REGEN with excitation densities of (a) 0.64 and (b) 2.02 mJ/cm<sup>2</sup>. A pump pulse of 330 nm was obtained from an OPA.

band overlapping the BX band and the biexcitons being scattered and annihilated by excitons, other biexcitons, and bound excitons.<sup>23,24</sup>

In summary, high-quality ZnO nanowires with high aspect ratios were synthesized at a MOCVD-growth temperature (550 °C) by means of assistance by colloidal Au nanoparticles dispersed on SiO<sub>2</sub>/Si substrates by a spin-coating technique. ZnO nanowires with diameters of 20–60 nm and lengths of 5–15 μm showed a high-internal quantum efficiency and negligibly weak deep-level emission in addition to a clearly observed EX band even at low temperatures (10–50 K) in PL measurements. These promising optical properties of MOCVD-grown ZnO nanowires can be attributed to the formation of an individual ZnO nanowire with a lower density of defects compared with that of a ZnO thin film and enlarged surface areas for emitting photons. The appearance of the BX band originating from the radiative recombination of biexcitons provides additional evidence that the ZnO nanowires in this study are of high quality.

The authors thank K. Kojima and M. Ueda for help in some of the experiments. This work was partly supported by Grants for Regional Science and Technology Promotion from the Ministry of Education, Culture, Sports, Science, and Technology of Japan.

- <sup>1</sup>A. Ohtomo, K. Tamura, M. Kawasaki, T. Makino, Y. Segawa, Z. K. Tang, G. K. L. Wong, Y. Matsumoto, and H. Koinuma, *Appl. Phys. Lett.* **77**, 2204 (2000).
- <sup>2</sup>M. H. Huang, S. Mao, H. Feick, H. Yan, Y. Wu, H. Kind, E. Weber, R. Russo, and P. Yang, *Science* **292**, 1897 (2001).
- <sup>3</sup>S.-W. Kim, Sz. Fujita, and Sg. Fujita, *Appl. Phys. Lett.* **81**, 5036 (2002).
- <sup>4</sup>Z. W. Pan, Z. R. Dai, and Z. L. Wang, *Science* **291**, 1947 (2001).
- <sup>5</sup>W. I. Park, Y. H. Jun, S. W. Jung, and G.-C. Yi, *Appl. Phys. Lett.* **82**, 964 (2003).
- <sup>6</sup>M. H. Huang, Y. Wu, H. Feick, N. Tran, E. Weber, and P. Yang, *Adv. Mater. (Weinheim, Ger.)* **13**, 113 (2001).
- <sup>7</sup>H. T. Ng, B. Chen, J. Li, J. Han, and M. Meyyappan, *Appl. Phys. Lett.* **82**, 2023 (2003).
- <sup>8</sup>B. D. Yao, Y. F. Chan, and N. Wang, *Appl. Phys. Lett.* **81**, 757 (2002).
- <sup>9</sup>B. Y. Geng, G. Z. Wang, Z. Jiang, T. Xie, S. H. Sun, G. W. Meng, and L. D. Zhang, *Appl. Phys. Lett.* **82**, 4291 (2003).
- <sup>10</sup>K. Maejima, M. Ueda, Sz. Fujita, and Sg. Fujita, *Jpn. J. Appl. Phys., Part 1* **42**, 2600 (2003).
- <sup>11</sup>J. Zhong, S. Muthukumar, Y. Chen, Y. Lu, H. M. Ng, W. Jiang, and E. L. Garfunkel, *Appl. Phys. Lett.* **83**, 3401 (2003).
- <sup>12</sup>S. H. Jo, J. Y. Lao, Z. F. Ren, R. A. Farrer, T. Baldacchini, and J. T. Fourkas, *Appl. Phys. Lett.* **83**, 4821 (2003).
- <sup>13</sup>In order to estimate the density of the MOCVD-grown ZnO nanowires on the substrate at 550 °C, the nanowires in Fig. 2(a) have been carefully examined. The density of the nanowires was approximately  $2 \times 10^9$  cm<sup>-2</sup>.
- <sup>14</sup>K. Ogata, T. Kawawishi, K. Maejima, K. Sakurai, Sz. Fujita, and Sg. Fujita, *Jpn. J. Appl. Phys., Part 2* **40**, L657 (2001).
- <sup>15</sup>I. Shalish, H. Temkin, and V. Narayanamurti, *Phys. Rev. B* **69**, 245401 (2004).
- <sup>16</sup>R. C. Miller, D. A. Kleinman, W. A. Nordland, Jr., and A. C. Gossard, *Phys. Rev. B* **22**, 863 (1980).
- <sup>17</sup>Y. Kawakami, Y. Narukawa, K. Omae, Sg. Fujita, and S. Nakamura, *Phys. Status Solidi A* **178**, 331 (2000).
- <sup>18</sup>A. van Dijken, J. Makkinje, and A. Meijerink, *J. Lumin.* **92**, 323 (2001).
- <sup>19</sup>S. Miyamoto and S. Shionoya, *J. Lumin.* **12-13**, 563 (1976).
- <sup>20</sup>B. P. Zhang, N. T. Binh, Y. Segawa, K. Wakatsuki, and N. Usami, *Appl. Phys. Lett.* **83**, 1635 (2003).
- <sup>21</sup>H. D. Sun, T. Makino, Y. Segawa, M. Kawasaki, A. Ohtomo, K. Tamura, and H. Koinuma, *Appl. Phys. Lett.* **78**, 3385 (2001).
- <sup>22</sup>R. T. Phillips, D. J. Lovering, and G. J. Denton, *Phys. Rev. B* **45**, 4308 (1992).
- <sup>23</sup>Y. Yamada, T. Mishina, Y. Masumoto, Y. Kawakami, J. Suda, Sz. Fujita, and Sg. Fujita, *Phys. Rev. B* **52**, R2289 (1995).
- <sup>24</sup>A. Yamamoto, K. Miyajima, T. Goto, H. J. Ko, and T. Yao, *J. Appl. Phys.* **90**, 4973 (2001).